

One-way catalysis: Insights from a solvable lattice model

Sara Mahdavi, Yann Sakref, and Olivier Rivoire

Gulliver, ESPCI, CNRS, Université PSL, Paris, France

Catalysts speed up chemical reactions with no energy input and without being transformed in the process, therefore leaving equilibrium constants unchanged. Some catalysts, however, are much more efficient at accelerating one direction of a reaction. How is such an asymmetry consistent with chemical equilibrium, where as many forward and reverse reactions must occur? We use the rigorous framework of a simple but exactly solvable lattice model to study this question in the context of a strictly one-way catalyst, which can only accelerate one way of a reaction. The model illustrates a mathematical relationship between asymmetric transition rates, which underlie directional catalysis, and symmetric transition fluxes, which underlie chemical equilibrium. The degree of directionality generally depends on the catalytic mechanism and we compare different mechanisms to show how they can obey different scaling laws. The results showcase the ability of simple physical models to address fundamental questions in catalysis.

I. INTRODUCTION

Catalysis, the acceleration of chemical reactions by substances that remain unchanged, is central to biological processes as well as the chemical industry. It also plays a key role in many non-equilibrium phenomena studied in statistical physics, from molecular motors to active matter. In these contexts, catalysis is most often treated phenomenologically by imposing kinetic rates without considering the microscopic interactions that underlie them. This allows one to ignore the chemical mechanisms by which catalysis operates, but at the cost of leaving aside any question pertaining to the physical limitations of these mechanisms.

To address such questions, we have previously introduced simplified models of catalysis in which the kinetic states and rates of a catalytic cycle are derived from a microscopic description of interacting particles [1–3]. A first class of models, in which the catalyst consists of rigidly held particles, reproduces two general principles of chemical catalysis [1, 2]: Pauling’s principle stating that the geometry of an optimal catalyst should be complementary to the transition state of the reaction [4], and Sabatier’s principle stating that the interaction between the reactants and the catalyst should be neither too weak nor too strong [5]. For this class of models, we found that catalysis can only lower the activation barrier of a reaction by a finite factor [3], consistent with observations in chemistry [6]. A second class of models, in which the catalyst can switch between two internal states, reproduces the ability of enzymes to overcome this limitation by an allosteric mechanism [3, 6].

Here we apply and extend our approach to examine a very basic question: if a substance is a catalyst for one direction of a reaction, is it necessarily a catalyst for the opposite direction of the same reaction? Since catalysis involves no energy input, it does not affect the equilibrium properties and it may therefore seem that catalysis is necessarily symmetrical, otherwise the second principle of thermodynamics would be violated. This conclusion is supported by the simple explanation of catalysis as the lowering of activation energies, which is often taken as an argument for universal bidirectionality [7–9]. Yet, many catalysts are

known to preferentially accelerate one direction of a reaction [10]. In the context of enzymes, it has been repeatedly noted that such one-way catalysis does not contradict any fundamental principle: catalysts accelerate only reactions that are thermodynamically favorable, and the two directions of a reaction are favorable under different conditions [10]. The conditions under which catalysis of one direction or the other of a reaction is observed are simply not comparable. This conclusion is borne out mathematically by analyzing the consequences of the reversible Michaelis-Menten equation [11]. However, these arguments do not reveal what happens at the microscopic level of individual molecules, where the same catalytic mechanisms must be at work regardless of the macroscopic conditions. In particular, at chemical equilibrium, while the relative concentration of reactants and products remains globally unchanged, the presence of catalysts must affect the frequency of transitions between reactants and products by the same factor. But how can such a symmetrical effect on the transition frequencies be reconciled with the preferential acceleration of one direction of the reaction?

To clarify this point, we draw on two elements of our previous work. First, we study catalysis in the framework of a simple lattice model that can be solved without approximation by exact numerical calculations and, in particular cases, analytical calculations [3]. We analyze the simplest reaction that can be defined in this framework: the dissociation or association of two particles interacting with a short-range potential. Second, we apply a quantitative definition of catalysis based on first-passage times [2, 12, 13], which we have shown to be consistent with other common definitions [14]. This allows us to study catalysis at the single-molecule level, with a clear criterion for asserting whether catalysis is or is not taking place.

Using these approaches, we show how any confusion can be dispelled by distinguishing between reaction *fluxes*, which depend on macroscopic conditions and are symmetric at chemical equilibrium, and reaction *rates*, which are independent of macroscopic conditions and are generally asymmetric. In particular, we show that it is possible to have strictly one-way catalysis, where the rate of one side of a reaction is accelerated but not the other. The demonstration is based on a reaction that has two activation barriers of different nature, energetic and entropic. This leads us to examine how different catalytic mechanisms are suitable for different types of activation barriers, and how they exhibit different scaling laws as a function of the amplitude of these activation barriers.

II. METHODS

For the sake of completeness, we first present the modeling framework on which we rely, first introduced in [3]. A compendium of useful mathematical formulas is provided in the Appendices.

A. Microscopic model

We consider a model of particles occupying the sites of a two-dimensional hexagonal lattice with periodic boundary conditions along one direction, as shown in Fig. 1A. We restrict our study to two non-overlapping particles that can diffuse from one site to the next and form a dimer when they are close together. The interaction between the particles is determined by the potential shown in Fig. 1B, which depends only on the distance d between

the two particles, measured by the minimum number of sites separating them. Particles at distance $d = 1$ are in a stable bound state, particles at distance $d \geq 3$ are non-interacting, while particles at distance $d = 2$ are in an unstable transition state. The potential has two parameters: a dissociation barrier h_s^+ and an association barrier h_s^- (Fig. 1B). A configuration $x = (i_1, i_2)$ with the two particles at positions i_1 and i_2 thus has an interaction energy given by

$$E_s(i_1, i_2) = \begin{cases} +\infty & \text{if } d(i_1, i_2) = 0 \\ h_s^- - h_s^+ & \text{if } d(i_1, i_2) = 1 \\ h_s^- & \text{if } d(i_1, i_2) = 2 \\ 0 & \text{if } d(i_1, i_2) \geq 3 \end{cases} \quad (1)$$

A rigid and fixed catalyst C is defined by assigning to some sites $\mathcal{S} = \{j_1, \dots, j_n\}$ of the lattice binding energies $\epsilon_{cs}^{j_1}, \dots, \epsilon_{cs}^{j_n}$ such that when a particle occupies site j_k , its energy is lowered by $\epsilon_{cs}^{j_k}$. As shown in previous works [1–3], the simplest configuration providing catalysis consists of two binding sites at distance $d = 2$ with a common binding energy ϵ_{cs} , for example $\mathcal{S} = \{1, 3\}$ (red sites in Fig. 1A) with $\epsilon_{cs}^1 = \epsilon_{cs}^3 = \epsilon_{cs}$. In general, the total energy of the configuration $x = (i_1, i_2)$ is

$$E(i_1, i_2) = E_s(i_1, i_2) - \sum_{j \in \mathcal{S}} (\epsilon_{cs}^j \delta_{j, i_1} + \epsilon_{cs}^j \delta_{j, i_2}) \quad (2)$$

where $\delta_{j, i_k} = 1$ if $i_k = j$ and 0 otherwise.

As a result of thermal fluctuations, transitions can occur from one configuration x of the particles to another y where one of the particles has moved to a neighboring site. Formally, if $x = (i_1, i_2)$, we can have either $y = (i'_1, i_2)$ with $d(i'_1, i_1) = 1$ and $d(i'_1, i_2) > 0$, or $y = (i_1, i'_2)$ with $d(i'_2, i_2) = 1$ and $d(i'_2, i_1) > 0$. We assume that the transitions occur at a rate given by

$$\rho(x \rightarrow y) = \rho_0 \min(1, e^{-\beta(E(y) - E(x))}) \quad (3)$$

where ρ_0 defines a diffusion rate, which we set to 1 in the following, and where $\beta = 1/(k_B T)$ is the inverse of the temperature multiplied by the Boltzmann constant. This choice of transition rates, which corresponds to Metropolis rule, satisfies the detailed equilibrium and thus ensures that the system asymptotically reaches an equilibrium distribution given by the Boltzmann law, where the probability $\pi(x)$ of being in the configuration x is proportional to $e^{-\beta E(x)}$.

To sum up, the parameters of the model include the geometry of the lattice, which we take to be of dimension $L \times L$ ($L = 6$ in Fig. 1A), the two activation energies h_s^+ and h_s^- for the spontaneous reaction, the choice of the binding sites \mathcal{S} and their energies ϵ_{cs}^j which define a putative catalyst, and the inverse temperature β . While the latter could be fixed to 1 without loss of generality, it is convenient to keep it as an explicit parameter to study scaling laws in the limit of a low temperatures ($\beta \rightarrow \infty$). Unless otherwise mentioned, we take $h_s^+ = 1$, $h_s^- = 2$, $\epsilon_{cs} = 1/2$ and $\beta = 10$ for the figures.

B. Definition and quantification of catalysis

Following [2, 3, 14], we define and quantify catalysis by the mean first-passage time to complete a reaction. We focus first on the cleavage reaction by which a dimer of two particles at distance $d = 1$ dissociates into two free particles at distance $d \geq 3$. To formally define this reaction, we collect all configurations in which the particles form a dimer that does

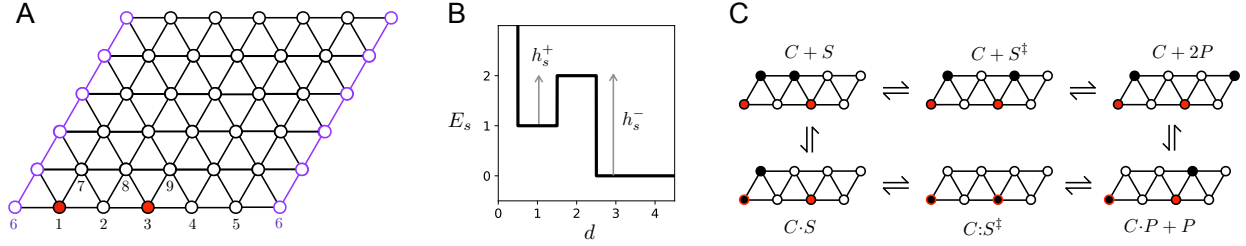


FIG. 1: Model definition. **A.** A two-dimensional lattice of size $L \times L$ with periodic boundary conditions along the x axis (repeated purple nodes). A particle can occupy any site on the lattice that is not already occupied by another particle. The sites are labeled $i = 1, \dots, L^2$. Some sites $\mathcal{S} = \{j_1, \dots, j_n\}$, e.g. $\mathcal{S} = \{1, 3\}$ shown in red, are defined as binding sites with associated binding energies ϵ_{CS}^{jk} . If a particle is at the binding site j_k , the energy is lowered by ϵ_{CS}^{jk} . **B.** The potential of interaction between two particles. This potential is defined by the distance d between the two particles, measured by the minimal path separating them. Particles at distance $d = 1$ are in a bound state, and particles at distance $d \geq 3$ are in a free state. The potential is parameterized by the two activation energies h_s^+ and h_s^- . Here $h_s^+ \leq h_s^-$, but the opposite is also possible. **C.** Configurations representing the different states along a catalytic cycle for the case of a catalyst consisting of two binding sites at distance $d = 2$. The top configurations, where the particles do not occupy the binding sites, represent the spontaneous reaction. The lower configurations represent the states with an interaction with the catalyst: $C \cdot S$ corresponds to a bound state with a particle on a binding site, $C \cdot S^\ddagger$ to a transition state with the two binding sites occupied, and $C \cdot P + P$ to a free state with a particle on a binding site.

not interact with the catalyst, i.e., configurations $x = (i_1, i_2)$ with $d(i_1, i_2) = 1$ and $i_1, i_2 \notin \mathcal{S}$ into a macrostate $C + S$, and all configurations where the two particles are free and not interacting with the catalyst, i.e., configurations $x = (i_1, i_2)$ with $d(i_1, i_2) \geq 3$ and $i_1, i_2 \notin \mathcal{S}$ into a macrostate $C + 2P$. A catalyzed reaction, denoted $C + S \rightarrow C + 2P$, corresponds to a transition from a configuration in $C + S$ to a configuration in $C + 2P$. Starting from a given configuration x in $C + S$, the time to first reach a configuration in $C + 2P$ is stochastic. The average time over stochastic trajectories defines the mean first-passage time $T_{x \rightarrow C+2P}$. Further averaging over the configurations x in $C + S$ defines the global mean first-passage time $T_{C+S \rightarrow C+2P}$.

When all interaction energies are zero, this mean first-passage time indicates the mean time to complete the spontaneous reaction and is simply denoted $T_{S \rightarrow P}$ [25]. We say that a particular choice of interaction energies defines a catalyst if $T_{C+S \rightarrow C+2P}$ is less than $T_{S \rightarrow 2P}$. The ratio between these two times, denoted $\eta_{C+S \rightarrow C+2P} = T_{S \rightarrow 2P} / T_{C+S \rightarrow C+2P}$, which must be > 1 for catalysis to occur, quantifies the catalytic efficiency. We have previously shown how this definition of catalysis is consistent with other definitions in chemistry and enzymology, and how, for the particular cleavage reaction $S \rightarrow 2P$, performing the analysis with two particles is sufficient to cover catalysis with more particles [14].

C. Calculations

Several approaches are available to compute mean first-passage times and thus verify whether a particular choice of binding sites and their interaction energy defines a catalyst. One possibility is to perform numerical simulations of stochastic trajectories using a kinetic Monte Carlo algorithm [15]. This approach is not exact, but it is very general. The main difficulty is that the time for the simulations diverges with increasing values of β . Alternative numerical approaches have been developed to get around this problem [16]. Here we follow [3] and compute the mean first passage directly by algebraic manipulation of the transition matrix of the associated Markov process, which amounts to directly solving the master equation (see Appendices). This approach is exact to numerical precision, but is only suitable for relatively small lattice sizes, since it involves inverting a matrix whose size scales with the total number of configurations. If L^2 is the number of lattice sites, then the number of different configurations x is indeed $N = L^2(L^2 - 1)$, which scales as L^4 . Since the conceptual questions that we are investigating are defined independently of the lattice size, we take $L = 6$ here, which allows us to make this approach tractable.

Using this approach, we obtain $\eta_{C+S \rightarrow C+2P} = T_{S \rightarrow 2P} / T_{C+S \rightarrow C+2P}$ for a putative catalyst consisting of two binding sites, $\mathcal{S} = \{1, 3\}$ with a common interaction energy ϵ_{cs} . The results lead to several observations [3] (Fig. 2). First, catalysis ($\eta_{C+S \rightarrow C+2P} > 1$) occurs only for sufficiently small values of the interaction strength ϵ_{cs} and sufficiently large values of the reverse activation barrier h_s^- . Second, catalysis is optimal when ϵ_{cs} takes an intermediate value and when h_s^- is maximal. Finally, $\eta_{C+S \rightarrow C+2P}$ scales exponentially with β , with an exponent that can be determined analytically (see Appendix A). As we will see, this exponent quantifies the catalytic efficiency of different mechanisms independently of their geometric peculiarities. It has a simple physical interpretation in terms of activation energy. For example, if we consider the spontaneous reaction $S \rightarrow 2P$ with activation energy h_s^+ , such that for large β , $T_{C+S \rightarrow C+2P} \sim e^{-\beta h_s^+}$, we generally expect $T_{C+S \rightarrow C+2P} \sim e^{-\beta a h_s^+}$, where $a < 1$ represents the factor by which the catalyst reduces the activation energy. The smaller a , the more efficient the catalysis, with $a = 0$ representing perfect or diffusion-limited catalysis, where energetic barriers are effectively eliminated. Given such a scaling, $\eta_{C+S \rightarrow C+2P} \sim e^{(1-a)h_s^+}$.

III. RESULTS

A. One-way catalysis

Is a catalyst for one reaction necessarily a catalyst for the reverse reaction? As such, the question may be considered ill-posed, since catalysis is not an intrinsic property of the catalyst, but depends on the extrinsic conditions under which it operates, which include, for example, temperature and substrate and product concentrations [14]. However, we can ask whether a molecule can act as a catalyst for a reaction under certain extrinsic conditions, while never acting as a catalyst for the reverse reaction under any extrinsic conditions.

The design considered so far, consisting of two binding sites at a distance of $d = 2$, shows bidirectionality for most binding energies. It catalyzes dissociation $S \rightarrow 2P$ and reverse dimerization $2P \rightarrow S$ over nearly the same range of interaction strengths ϵ_{cs} (Fig. 3A), although it is possible to find values of ϵ_{cs} , e.g. $\epsilon_{cs} = 1$, for which (weak) forward catalysis occurs ($\eta_{C+S \rightarrow C+2P} > 1$) but not reverse catalysis ($\eta_{C+2P \rightarrow C+S} < 1$). Changing the geometry of the binding sites to form four consecutive binding sites, $\mathcal{S} = \{1, 2, 3, 4\}$ with the sites labeled

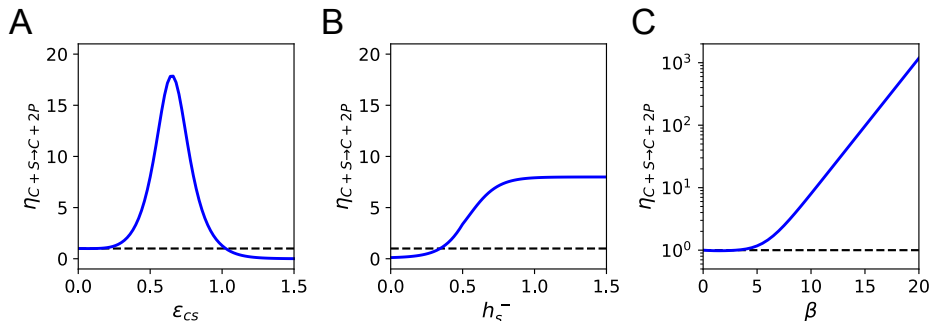


FIG. 2: Catalytic efficiency $\eta_{C+S \rightarrow C+2P}$ for a catalyst consisting of two sites at distance $d = 2$, here shown for $h_s^+ = 1$, $h_s^- = 2$, $\epsilon_{cs} = 1/2$ and $\beta = 10$, unless one of these parameters is varied. **A.** Dependence on the interaction ϵ_{cs} , showing a maximum at an intermediate value of ϵ_{cs} . This graph is analogous to Volcano plots drawn from empirical data in heterogeneous catalysis and reflects the Sabatier principle [17]: too weak an interaction is insufficient to accelerate the chemical step $C \cdot S \rightarrow C \cdot P + P$, while too strong an interaction prevents efficient release $C \cdot P + P \rightarrow C + 2P$. The dashed black line indicates the threshold $\eta_{C+S \rightarrow C+2P} = 1$ above which catalysis occurs. **B.** Dependence on the reverse activation energy h_s^- , showing that catalysis requires a sufficiently large value of h_s^- and that catalytic efficiency saturates at large values of h_s^- . **C.** Catalytic efficiency as a function of inverse temperature β , showing exponential scaling. The exponent is given by $1 - a$ where a is given in Eq. (A1).

as in Fig. 1A, provides a more striking example of one-way catalysis. As shown in Fig. 3F, forward catalysis is never observed ($\eta_{C+S \rightarrow C+2P} < 1$ for any ϵ_{cs}), while reverse catalysis is observed ($\eta_{C+2P \rightarrow C+S} > 1$ for some ϵ_{cs}).

The difference is due to the different nature of the forward and backward kinetic barriers of the spontaneous reaction. The forward reaction $S \rightarrow 2P$ is limited by a purely energetic barrier. To accelerate this reaction, a catalyst must specifically stabilize the transition state S^\ddagger of the reaction, when the two particles are at a distance $d = 2$ (Fig. 2B). This is achieved with two binding sites separated by exactly the distance between the particles in the transition state: the total interaction energy is $2\epsilon_{cs}$ for the transition state complex CS^\ddagger , while it is only ϵ_{cs} for CS and CP (Fig. 2C). This mechanism of “strain catalysis” [18] follows Pauling principle [4], with a geometry complementary to the transition state. Now, in contrast, the four-site design cannot distinguish between the substrate S , the transition state S^\ddagger , and the product $2P$: all bind with the same total interaction energy $2\epsilon_{cs}$. On the other hand, the reverse reaction $2P \rightarrow S$ has both an energetic barrier, represented by h_s^- (Fig. 2B), and an entropic barrier, corresponding to the need for the two particles to diffuse toward each other. While a patch of four binding sites cannot lower the energetic barrier, it can lower the entropic barrier by keeping the two particles in close proximity until they cross the energetic barrier. This mechanism of catalysis by proximity does not require any special geometry but applies only to multi-reactant reactions and is therefore only effective for the reverse reaction $2P \rightarrow S$.

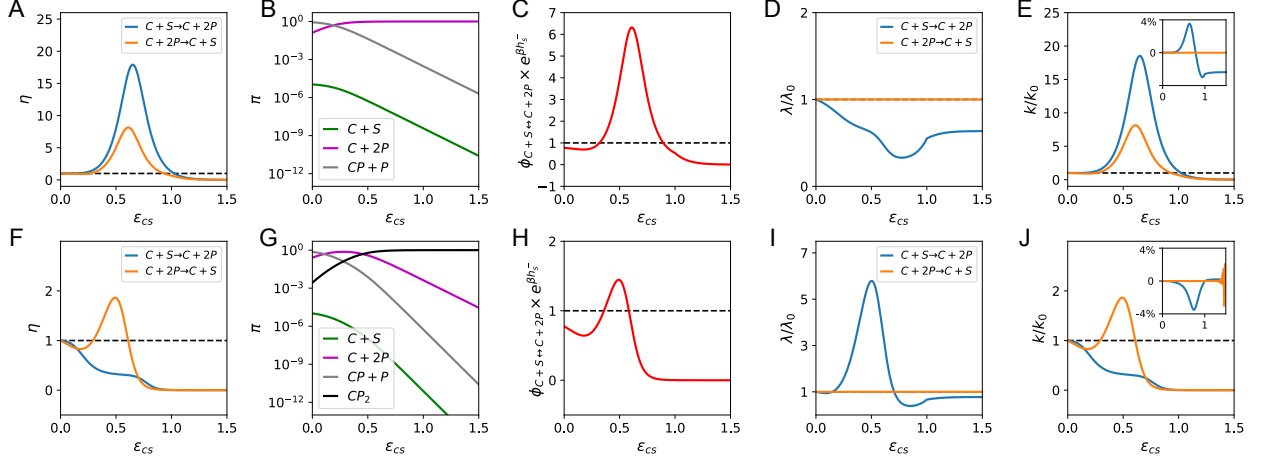


FIG. 3: Forward versus reverse catalysis with a two-site (top row) or four-site (bottom row) catalyst. **A.** $\eta_{C+S \rightarrow C+2P}$ (in blue) versus $\eta_{C+2P \rightarrow C+S}$ (in orange), showing comparable behavior as a function of interaction strength ϵ_{cs} . **B.** Steady-state concentrations of the three macrostates $C+S$, $C+2P$, and $CP+P$, showing a constant ratio π_{C+S}/π_{C+2P} , consistent with an unchanged equilibrium constant. **C.** Steady-state flux $\phi_{C+S \rightarrow C+2P}$ at which transitions occur between $C+S$ and $C+2P$ (rescaled by the constant factor $e^{\beta h_s^-}$ to be of order one). **D.** Steady-state probabilities $\lambda_{C+S \rightarrow C+2P}$ (in blue) and $\lambda_{C+2P \rightarrow C+S}$ (in orange) for the system to be on its way from $C+S$ to $C+2P$ or from $C+2P$ to $C+S$, normalized to their values λ_0 when $\epsilon_{cs} = 0$. Although not visible in this representation of relative variations, both quantities vary by the same absolute amount, since $\lambda_{C+S \rightarrow C+2P} + \lambda_{C+2P \rightarrow C+S} = 1$ for any value of ϵ_{cs} . **E.** Catalytic rates $k_{C+S \rightarrow C+2P} = \phi_{C+S \rightarrow C+2P}/\lambda_{C+S \rightarrow C+2P}$ (in blue) and $k_{C+2P \rightarrow C+S} = \phi_{C+2P \rightarrow C+S}/\lambda_{C+2P \rightarrow C+S}$ (in orange). Normalized to their values k_0 when $\epsilon_{cs} = 0$, these rates coincide within a few percent with $\eta_{C+S \rightarrow C+2P}$ and $\eta_{C+2P \rightarrow C+S}$ (relative difference shown in inset). **F-G** Comparable plots for a system with four consecutive binding sites. The main difference is that catalysis is only observed in the opposite direction, with $\eta_{C+S \rightarrow C+2P} < 1$ for all values of ϵ_{cs} (panel F).

B. Catalysis at thermal equilibrium

How is the observation of one-way catalysis consistent with thermodynamic principles? Indeed, one-way catalysis is often ruled out on the basis that catalysis does not change the equilibrium constant and therefore must accelerate both sides of a reaction equally [7]. To clarify this point, here we analyze our models under steady-state conditions that reproduce equilibrium properties.

Chemical equilibrium is usually associated with a specific ratio of the concentrations of substrates and products, known as the equilibrium constant. For the reaction $S \rightleftharpoons 2P$ studied so far, chemical equilibrium is thus characterized by $[S]/[P]^2 = e^{h_s^+ - h_s^-}$. This criterion is valid for systems with a large number of molecules whose concentrations are not affected by stochastic fluctuations. In the single-molecule context in which we analyze our model, we can instead invoke the ergodic principle to characterize chemical equilibrium by the ratio π_S/π_{2P} of the steady-state probabilities of the macrostates S and $2P$. The steady state probabilities π_S and π_{2P} are straightforward to calculate for our small system (Appendix C) and we verify that the presence of binding sites preserves the chemical equilibrium, $\pi_{C+S}/\pi_{C+2P} = \pi_S/\pi_P$,

independent of the geometry of the binding sites or the interaction strength ϵ_{cs} (Fig. 3B,G). However, the values of π_{C+S} and π_{C+2P} change with ϵ_{cs} as other alternative macrostates involving interactions with the binding sites are populated (Fig. 3B,G).

While catalysis does not affect the relative occurrence of free substrates and free products at steady state, it does affect the flux between these states, i.e. the frequency with which two particles go from a free dimer (macrostate $C+S$) to two free particles (macrostate $C+2P$). For any Markov process, the steady state flux from one macrostate A to another macrostate B is the frequency at which the system first reaches B after visiting A . Since there must be as many transitions from A to B as from B to A at steady state, the flux is symmetric with $\phi_{A \rightarrow B} = \phi_{B \rightarrow A}$, which justifies denoting it by $\phi_{A \leftrightarrow B}$. Applied to $A = C+S$ and $B = C+2P$, this symmetry captures the intuition that a catalyst has a symmetrical incidence on the two directions of a reaction. Fluxes can be computed exactly for our small system (Appendix C). We find that the flux $\phi_{C+S \leftrightarrow C+2P}$ depends non-trivially on the interaction strength ϵ_{cs} with a maximum at an intermediate value of ϵ_{cs} , for both the two-site and the four-site designs (Fig. 3C-H).

To clarify how a symmetric flux $\phi_{A \leftrightarrow B}$ between two macrostates A and B relates to asymmetric mean first-passage times $T_{A \rightarrow B}$ and $T_{B \rightarrow A}$, one must consider the steady state probabilities $\lambda_{A \rightarrow B}$ and $\lambda_{B \rightarrow A}$ that the system is in the process of transitioning from A to B or from B to A [19]. Formally, $\lambda_{A \rightarrow B}$ is the steady-state probability that the system last visited A and not B , and similarly for $\lambda_{B \rightarrow A}$. These transition probabilities can again be computed exactly (Appendix C). $\lambda_{A \rightarrow B}$ and $\lambda_{B \rightarrow A}$ are generally different, but directly related: at any given time, the system either transitions from A to B or from B to A , so that $\lambda_{A \rightarrow B} + \lambda_{B \rightarrow A} = 1$. Combining the flux $\phi_{A \leftrightarrow B}$ and the transition probability $\lambda_{A \rightarrow B}$ leads to the definition of the rate $k_{A \rightarrow B}$ at which a system in A transitions to B , given by $k_{A \rightarrow B} = \phi_{A \rightarrow B} / \lambda_{A \rightarrow B}$ [19]. If the Markov process is reversible, $k_{A \rightarrow B} \simeq 1/T_{A \rightarrow B}$, to the extent that A and B define stable Markov states [20]. More precisely, the mean first-passage times $T_{A \rightarrow B}$ and $T_{B \rightarrow A}$ are related to the flux $\phi_{A \leftrightarrow B}$ by $\phi_{A \rightarrow B} \simeq 1/(T_{A \rightarrow B} + T_{B \rightarrow A})$ and $\lambda_{A \rightarrow B} \simeq T_{A \rightarrow B}/(T_{A \rightarrow B} + T_{B \rightarrow A})$ [20]. These general mathematical relationships explain how the maintenance of equilibrium properties, which is a matter of *flux*, can be consistent with asymmetric catalysis, which is a matter of *rates*, with the general relation

$$\phi_{C+S \leftrightarrow C+2P} \simeq k_{C+S \rightarrow C+2P} \lambda_{C+S \rightarrow C+2P} \simeq k_{C+2P \rightarrow C+S} \lambda_{C+2P \rightarrow C+S} \quad (4)$$

Calculating $\lambda_{C+S \rightarrow C+2P}$ and $\lambda_{C+2P \rightarrow C+S}$ for the two binding site geometries considered so far, we find that $\lambda_{C+S \rightarrow C+2P}$ undergoes large relative changes when ϵ_{cs} is varied, but not $\lambda_{C+2P \rightarrow C+S}$ (Fig. 3D,I). Both, however, undergo the same absolute changes since $\lambda_{C+S \rightarrow C+2P} + \lambda_{C+2P \rightarrow C+S} = 1$. The difference is that $\lambda_{C+S \rightarrow C+2P} \gg \lambda_{C+2P \rightarrow C+S}$ as a consequence of the parameters chosen in Fig. 3, which favor $C+2P$ over $C+S$ since $e^{-\beta h_s^-} \ll e^{-\beta h_s^+}$. Using the ratio of $\phi_{C+S \leftrightarrow C+2P}$ over $\lambda_{C+S \rightarrow C+2P}$ or $\lambda_{C+2P \rightarrow C+S}$ to estimate the rates $k_{C+S \rightarrow C+2P}$ and $k_{C+2P \rightarrow C+S}$, we verify $k_{C+S \rightarrow C+2P}/k_{S \rightarrow 2P} \simeq \eta_{C+S \rightarrow C+2P}$ and $k_{C+2P \rightarrow C+S}/k_{2P \rightarrow S} \simeq \eta_{C+2P \rightarrow C+S}$ (Fig. 3A,E,F,J), consistent with the general arguments above. For the models and parameters of Fig. 3, the approximation holds within 4% (insets of Fig. 3E,J). Since the small discrepancy arises from the fact that $C+S$ and $C+2P$ are not strictly Markov states, it can be seen as a quantification of the validity of a coarse-grained description by a Markov model with states $C+S$ and $C+2P$ (see Appendix B).

In addition to clarifying how one-way catalysis is consistent with preserving chemical equilibrium, the mathematical relationship between rates and first passage times illustrated by the correspondence between Fig. 3A,F and Fig. 3D,I implies that we can in principle detect and quantify catalysis from equilibrium trajectories.

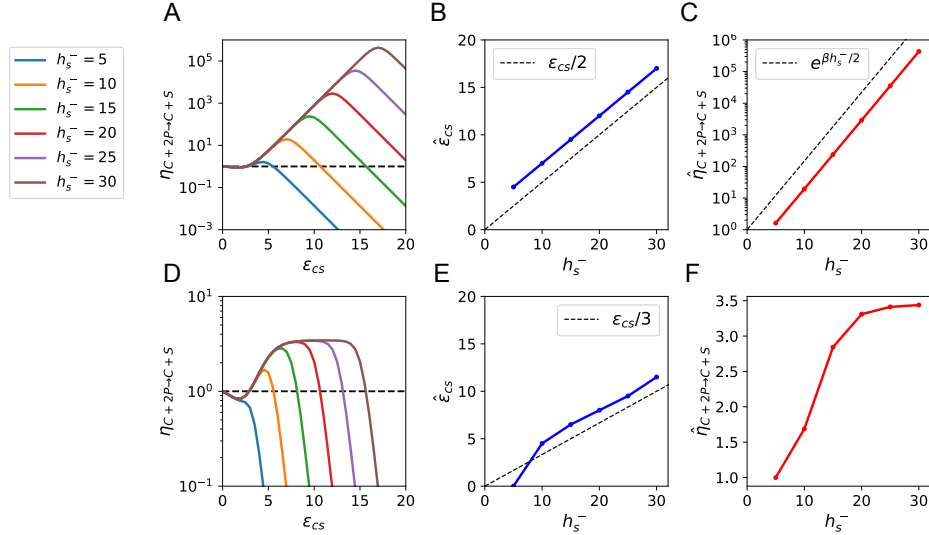


FIG. 4: Low temperature scaling laws for the catalysis of the dimerization reaction $2P \rightarrow S$ for a two-site (top row) or a four-site (bottom row) catalyst. **A.** Catalytic efficiency $\eta_{C+2P \rightarrow C+S}$ as a function of interaction strength ϵ_{cs} for different activation barriers h_s^- , showing the shape of a Volcano plot as for the opposite reaction $S \rightarrow 2P$ (Fig. 2A). **B.** Scaling of the optimal interaction strength ϵ_{cs} as a function of h_s^- . The dashed line has a slope of $1/2$, indicating a scaling of $\epsilon_{cs} \sim h_s^-/2$. **C.** Scaling of the optimum of $\eta_{C+2P \rightarrow C+S}$ when varying ϵ_{cs} as a function of h_s^- , showing a scaling $\eta_{C+2P \rightarrow C+S} \sim e^{\beta h_s^-}$. **D.** As in A, but for four consecutive binding sites (note the different scale on the y-axis). With four consecutive binding sites, **E.** the optimal interaction strength ϵ_{cs} scales as $h_s^-/3$ and **F.** the optimal catalytic efficiency saturates at large values of h_s^- .

C. Entropic versus strain catalysis

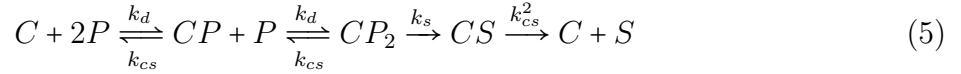
The two-site and four-site geometries are two alternative designs for catalyzing the dimerization reaction $2P \rightarrow S$, using different mechanisms: the four-site system relies only on catalysis by proximity, while the two-site system involves a specific stabilization of the transition state. Here we compare the efficiency of these two mechanisms by extending the scaling analysis previously performed for the two-site catalysis of the cleavage reaction $S \rightarrow 2P$ [3] (see Appendix A).

Fig. 4 shows that the two mechanisms have different scaling laws in the low temperature limit. With the two-site system we recover the conclusions obtained with the forward reaction $S \rightarrow 2P$ [3]: the optimal interaction strength scales with the activation energy, here h_s^- , as $\epsilon_{cs} = h_s^-/2$, leading to an optimal catalytic efficiency $\eta_{C+2P \rightarrow C+S}$ that increases with h_s^- as $\eta_{C+2P \rightarrow C+S} \sim e^{\beta h_s^-/2}$ (see Appendix A). As for the forward reaction, the activation energy is reduced by a factor of 2 at most. For the four-site system, however, we observe that the optimal interaction strength scales with the activation energy h_s^- as $\epsilon_{cs} \sim h_s^-/3$ and that the optimal catalytic efficiency $\eta_{C+2P \rightarrow C+S}$ reaches a plateau as h_s^- increases (Fig. 3D-F).

The scaling laws for the catalysis of the dimerization reaction $2P \rightarrow S$ by the two-site system are explained by the same arguments that we used for the catalysis of the dissociation reaction $S \rightarrow 2P$ [3] (see Appendix A). These arguments are based on the assumption that the diffusion is effectively instantaneous at low temperature, where crossing the highest

energy barrier is the limiting process. However, this assumption cannot be made when considering the catalysis of $2P \rightarrow S$ by four consecutive binding sites, since the time it takes two particles to diffuse toward each other is precisely what the four-site catalyst reduces.

To understand what limits catalysis in this case, we must consider the total area $V = L^2$ of the lattice as a parameter, since this is the parameter that controls the time spent diffusing. The coarse-grained model (see Appendix B) that captures the phenomenology in the $h_s^+ \gg h_s^-$ limit is of the form



where k_d is a diffusion constant that scales with volume as $k_d \sim 1/V$, k_{cs} is a dissociation rate that scales as $k_{cs} \sim e^{-\beta\epsilon_{cs}}$, and k_s is the rate at which the activation barrier h_s^- is crossed when the two reactants are close together that scales as $k_s \sim e^{-\beta h_s^-}$. Neglecting the spontaneous reaction, we can apply the general formula for mean first-passage times of one-dimensional Markov chains (Appendix C) to obtain

$$T_{C+2P \rightarrow C+S} = \frac{2}{k_d} + \frac{1}{k_s} + \frac{1}{k_{cs}^2} + \frac{k_{cs}}{k_d^2} + \frac{k_{cs}}{k_d k_s} + \frac{k_{cs}^2}{k_d^2 k_s}. \quad (6)$$

In the low temperature limit, where k_s is small, the optimal value of k_{cs} is determined by $1/k_{cs}^2 + k_{cs}/k_d k_s$, whose maximum is obtained when $k_{cs} \sim k_s^{1/3}$; this explains the scaling of the optimal ϵ_{cs} as $h_s^-/3$ in Fig. 4E. In the same limit, however, the value of $T_{C+2P \rightarrow C+S}$ is dominated by $2/k_d + 1/k_s$, which is independent of ϵ_{cs} ; this explains the plateau in Fig. 4F and has a simple interpretation: catalysis by proximity is limited by the time for the reactants to find the catalyst ($2/k_d$) and the time for them to cross the activation energy when in proximity ($1/k_s$), which are independent of ϵ_{cs} .

Despite operating on different principles and exhibiting different scaling behaviors, the two-site and four-site systems both give rise to Volcano plots with an optimal interaction energy at a finite value (Fig. 4A,D), in accordance with the Sabatier principle [17]. However, the shape of these Volcano plots is different. In the case of the four-site system operating by catalysis by proximity, a plateau is observed that can be understood from the coarse-grained model: this plateau extends to $\sim h_s^-/2$, which marks a crossover between the dominance of the term $1/k_s$ and the term $1/k_{cs}^2$ in Eq. (6), occurring when $k_{cs} \sim k_s^{1/2}$. In summary, optimal catalysis by proximity require neither a fine-tuned geometry nor a fine-tuned interaction strength, unlike optimal strain catalysis. However, catalysis by proximity is generally much less efficient due to the fact that the entropic barrier it reduces is typically lower than the energetic barrier that strain catalysis reduces.

D. Optimal rigid catalysis

We have so far considered two geometries of the binding sites and found that for the forward reaction $S \rightarrow 2P$ only the two-site geometry, where the binding sites are separated by $d = 2$, can confer catalysis. In previous work [3], we showed that a single binding site cannot confer catalysis, nor can two sites at a distance different from the transition state geometry $d = 2$. We also showed that introducing asymmetry into the two-site system by allowing each binding site to have a different interaction energy does not provide any

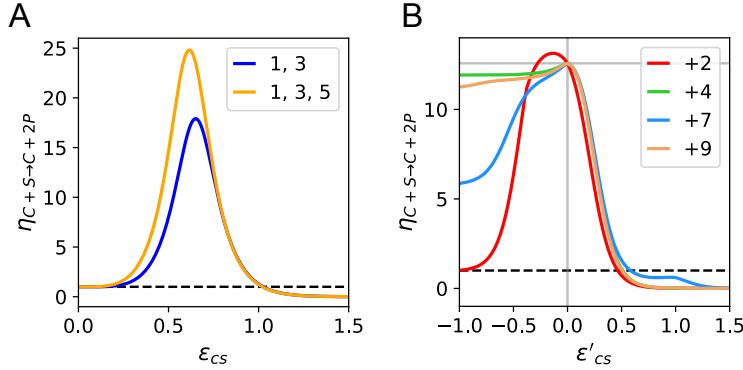


FIG. 5: Catalysis of the cleavage reaction $S \rightarrow 2P$ when a third binding site is introduced in addition to the two red binding sites shown in Fig. 1. **A.** Adding another site at $j = 5$ effectively increases the number of site pairs at distance $d = 2$ and thus provides an entropic improvement. For a fair comparison, $\eta_{C+S \rightarrow C+2P}$ is estimated by excluding from $C + S$ and $C + 2P$ all sites at the bottom of the lattice, which explains the slight difference of the blue curve from that of Fig. 2A. **B.** Addition of a third site at different positions next to one of the two binding sites at $j = 1$ and $j = 3$ (Fig. 1A). The labels indicate the third location where the binding site is added. Only when a third site is added between the other two (at $j = 2$) is a small improvement observed, for a destabilizing energy $\epsilon'_{cs} < 0$.

improvement. However, we can still wonder if a system with more than two sites, possibly with different interaction energies, can outperform a symmetric two-site system.

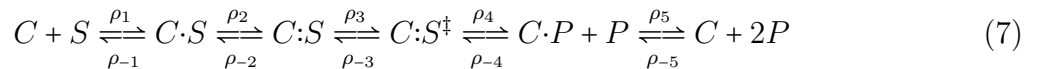
One possibility is to have more pairs of sites that implement the same mechanism of strain catalysis. For example, in the context of our 6×6 lattice, we can add a third binding site at $j = 5$ (Fig. 1A), which, given the periodic boundary conditions, provides 3 pairs of binding sites at distance $d = 2$. This model can be considered a model of heterogeneous catalysis, which typically involves a surface of periodically repeated binding sites. We verify that the additional binding site does provide an improvement (Fig. 5A), but this corresponds to an entropic factor that must leave the low-temperature scaling properties unchanged, in particular the factor a that controls the scaling of the catalytic efficiency $\eta_{C+S \rightarrow C+2P}$ with the amplitude of the activation energy (see Eq. (A1)).

Another question is whether it is possible to improve the two-site catalyst by adding a third binding site through a new or additional mechanism. As a systematic approach, we consider the addition of a third binding site at any site adjacent to one of the two binding sites at distance $d = 2$. The binding energy at this new site is taken to be ϵ'_{cs} , possibly different from the binding energy ϵ_{cs} at the two sites $j = 1$ and $j = 3$ (Fig. 1A). Considering the symmetries, four geometries are possible where the third binding site is located at sites $j = 2, 4, 7$ or 9 (Fig. 1A). We find that only in one case, when the third site is between the other two ($j = 2$), a small improvement is observed, provided that the interaction is repulsive, i.e. $\epsilon'_{cs} < 0$ (Fig. 5B).

First, we can understand why adding a third site at any other position is detrimental. Naively, a third site at $j = 4$, for example, can be thought of as favoring the release step $C \cdot P + P \rightarrow C + 2P$ by providing a “stepping stone” that replaces the crossing of a barrier ϵ_{cs} with the crossing of two smaller barriers whose sum is ϵ_{cs} . Strain catalysis essentially works like this: the barrier h_s^+ is replaced by two smaller barriers $h_s^+ - \epsilon_{cs}$ and ϵ_{cs} (see Eq. (A6)

with $h_s^+ \ll h_s^-$). As we noted, this mechanism only works in the presence of a reverse barrier $h_s^- > 0$. Simply replacing one barrier by two smaller ones in the absence of a reverse barrier never results in acceleration. Mathematically, using the formula for mean first-passage times of one-dimensional Markov processes (Appendix C) this amounts to replacing $T_{1 \rightarrow 2} = e^{-\beta \epsilon_{12}}$ by $T_{1 \rightarrow 3 \rightarrow 2} = e^{\beta \epsilon_{13}} + e^{\beta \epsilon_{32}} + e^{\beta(\epsilon_{13} + \epsilon_{32} - \epsilon_{32})}$ with the constraint $\epsilon_{13} + \epsilon_{32} = \epsilon_{12}$, which implies $T_{1 \rightarrow 3 \rightarrow 2} \geq T_{1 \rightarrow 2}$.

The same reasoning suggests that no benefit should be expected from a third binding site between the other two: introducing a “stepping stone” of intermediate energy cannot accelerate the transition from $C \cdot S \rightarrow C : S^\ddagger$. But if such a naive mechanism of “substrate destabilization” [10] cannot be effective, how to explain the (small) improvement observed in Fig. 1B? Denoting by $C : S$ the new state where S is bound to two consecutive sites ($i_1, i_2 = (1, 2)$ or $(2, 3)$), the catalytic cycle in the presence of a third middle binding site at $j = 2$, is described by a Markov chain of the form



If we first assume that the third site has zero binding energy ($\epsilon'_{cs} = 0$), we have $\rho_2 = \rho_{-2} = \rho_{-3} = \rho_4 = 1$ and the optimal interaction energy $\epsilon_{cs} = h_s^+/2$ for large β implies $\rho_3 = \rho_5$, leaving five equally dominant terms

$$T_{C+S \rightarrow C+2P} = \frac{1}{\rho_3} + \frac{1}{\rho_5} + \frac{\rho_{-2}}{\rho_2 \rho_3} + \frac{\rho_{-3}}{\rho_3 \rho_4} + \frac{\rho_{-2} \rho_{-3}}{\rho_2 \rho_3 \rho_4} \simeq 5e^{h^+/2} \quad (8)$$

By introducing a middle site with non-zero binding energy, the rate ρ_{-3} is changed to $\rho_{-3}e^{-\epsilon'_{cs}}$ and with $\epsilon'_{cs} < 0$ the two terms involving ρ_{-3} are no longer dominant, leading to $T_{C+S \rightarrow C+2P} \simeq 3e^{h^+/2}$. The factor $3/5$ is the gain observed in Fig. 1B. Physically, it is an entropic factor corresponding to a favored transition $C \cdot S \rightarrow C : S^\ddagger$, achieved by promoting a proper alignment of the substrate relative to the binding sites. As an entropic factor, it provides only a small improvement and has no effect on the low-temperature scaling behavior. In particular, a is still given by Eq. (A7), and the three-site catalyst is therefore subject to the same $a \geq 1/2$ limitation as the two-site catalyst [3].

IV. CONCLUSION

Fundamental thermodynamic principles dictate that catalysis, the acceleration of a reaction without any energy input or alteration of the catalyst, must preserve equilibrium properties. At first glance, this seems to exclude one-way catalysis where only one direction of a reaction is accelerated, since chemical equilibrium requires both directions of a reaction to occur with equal frequency. Similar to other apparent thermodynamic paradoxes related to irreversibility, the key issue lies in the initial conditions: catalysis is inherently tied to transformations that are defined by their starting and ending points. By definition, forward and reverse catalysis involve opposite starting and ending points. While arguments have already been made to justify the possibility of one-way catalysis [11, 21], revisiting the concept at the single-molecule level with a simple physical model provides additional insights. First, it provides a mathematical resolution to the paradox by distinguishing between two mathematical notions: transformation *rates*, which are asymmetric with respect to the two endpoints, and steady-state *fluxes*, which are symmetric at chemical equilibrium. In essence,

catalysis pertains to rates, while equilibrium pertains to fluxes. As shown in the context of our model, the two concepts are both distinct and simply mathematically related. In addition, the model demonstrates how both forward and reverse catalysis can be observed and quantified at the single-molecule level by following a single trajectory of successive forward and reverse reactions, with therefore a single initial condition.

Our example of strictly one-way catalysts, which can possibly accelerate only one direction of a reaction, relies on two features of the reaction and the catalyst. First, we considered a dimerization reaction $S \rightleftharpoons 2P$ in which the kinetic barriers limiting the forward and reverse directions are of different nature, namely purely energetic for dissociation and a mixture of energetic and entropic for association. Second, we studied a catalytic mechanism by proximity involving a patch of successive binding sites, which can possibly reduce only the entropic component of a reaction barrier. Since only the reverse direction of the reaction $S \rightleftharpoons 2P$ contains an entropic component, this mechanism can only accelerate this reverse direction. However, the fact that a catalyst is more efficient at catalyzing one direction of a reaction is very general and indeed generic, as illustrated by the other catalytic mechanism we studied, based on strain.

The distinction between two catalytic mechanisms, by proximity and by strain, led us to identify different scaling laws in the limit of large activation energies or, equivalently, small temperatures. However, we showed that for a given mechanism, the scaling of a catalyst with optimized interaction energies is robust to variations in its geometry. In particular, strain catalysis in our model can lower the activation barrier by a factor of at most two ($a \geq 1/2$), even when introducing more binding sites than the two required for minimal implementation of this mechanism. The additional sites can provide a small entropic improvement but do not change the optimal scaling. This limitation of strain catalysis is general and holds whenever the binding energies of the three reaction states – substrate S , transition state S^\ddagger , and product(s) $2P$ – are constrained to be correlated, which is generally caused by their chemical similarity [6]. In our specific model, the binding energy to the transition state is $2\epsilon_{cs}$, which cannot be increased without also increasing the binding energies to the substrate and product, both of which are ϵ_{cs} . If there is a different relationship between these three binding energies, the optimal scaling factor a can differ from $a = 1/2$, but a finite value $a > 0$ is expected as long as no internal degrees of freedom are introduced. As previously shown within the same modeling framework, this scaling can indeed be broken by replacing fixed binding sites with flexible ones, thus implementing a form of allostery commonly observed in enzymes [3].

Our modeling framework could be further generalized to address other questions related to catalysis, from fundamental questions in out-of-equilibrium thermodynamics to questions related to the origin of life. In theoretical treatments of these questions in the statistical physics literature, catalytic mechanisms have almost always been abstracted and treated only at the kinetic level. This is the case even when the focus is on studying specific enzymes, such as molecular motors, and when the models are intended to be mechanistic [22]. As shown here and in previous work [1–3, 23], catalytic mechanisms can be easily incorporated into simple and solvable physical models, allowing one to derive scaling laws and conceptual conclusions that are otherwise inaccessible.

Acknowledgments – We acknowledge funding from ANR-22-CE06-0037.

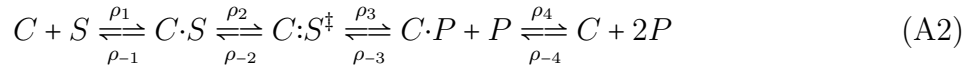
Appendix A: Low-temperature limit

The exponential scaling with β of the catalytic efficiency $\eta_{C+S \rightarrow C+2P}$ illustrated in Fig. 2C is consistent with Arrhenius law. For the spontaneous reaction we indeed have $T_{S \rightarrow 2P} \sim e^{\beta h_s^+}$, where the symbol \sim stands for $\lim_{\beta \rightarrow \infty} (\ln T_{S \rightarrow 2P})/\beta = h_s^+$. In the presence of catalysis, we can expect a similar scaling $T_{C+S \rightarrow C+2P} \sim e^{\beta a h_s^+}$ but with a factor $a < 1$ representing the reduction of the activation energy by the catalyst. More formally, we define this activation energy reduction by

$$a = \lim_{\beta \rightarrow \infty} \frac{\ln T_{C+S \rightarrow C+2P}}{\ln T_{S \rightarrow 2P}}. \quad (\text{A1})$$

With respect to this factor, $\eta_{C+S \rightarrow C+2P} \sim e^{\beta(1-a)h_s^+}$.

a can be calculated analytically by noting that, at low temperatures (large β), diffusion is much faster than barrier crossing. If we treat diffusion as instantaneous, or more precisely as occurring on the fastest time scale of the dynamics, which according to Eq. (3) is $1/\rho_0 = 1$, all configurations of the same energy connected by diffusion are effectively equivalent. For the model presented in Fig. 1, we have only five different states, $C + S$, $C \cdot S$, $C : S^\ddagger$, $C \cdot P + P$ and $C + 2P$ in this approximation (Fig. 1C), with respective energies $h_s^- - h_s^+$, $h_s^- - h_s^+ - \epsilon_{cs}$, $h_s^- - 2\epsilon_{cs}$, $-\epsilon_{cs}$ and 0, and the dynamics is reduced to a one-dimensional Markov chain between these states, of the form



We can then apply an analytical formula for the mean first passage times of one-dimensional Markov chains (see Appendix C)

$$T_{C+S \rightarrow C+2P} = \frac{1}{\rho_1} + \frac{1}{\rho_2} + \frac{1}{\rho_3} + \frac{1}{\rho_4} + \frac{\rho_{-1}}{\rho_1 \rho_2} + \frac{\rho_{-2}}{\rho_2 \rho_3} + \frac{\rho_{-3}}{\rho_3 \rho_4} + \frac{\rho_{-1} \rho_{-2}}{\rho_1 \rho_2 \rho_3} + \frac{\rho_{-2} \rho_{-3}}{\rho_2 \rho_3 \rho_4} + \frac{\rho_{-1} \rho_{-2} \rho_{-3}}{\rho_1 \rho_2 \rho_3 \rho_4} \quad (\text{A3})$$

If we consider $\epsilon_{cs} < h_s^+$, which is required for catalysis (otherwise release involves an activation energy ϵ_{cs} greater than the activation energy of the spontaneous reaction h_s^+), and assume for simplicity $\epsilon_{cs} < h_s^-$, an assumption which we show below to be nonrestrictive for optimal catalysis, we have

$$\rho_{-1} = e^{-\beta \epsilon_{cs}}, \quad \rho_2 = e^{-\beta(h_s^+ - \epsilon_{cs})}, \quad \rho_{-3} = e^{-\beta(h_s^- - \epsilon_{cs})}, \quad \rho_4 = e^{-\beta \epsilon_{cs}}, \quad \rho_1 = \rho_{-2} = \rho_3 = \rho_{-4} = 1. \quad (\text{A4})$$

These expressions result in

$$T_{C+S \rightarrow C+2P} = 2 + 2e^{\beta(h_s^+ - \epsilon_{cs})} + e^{\beta \epsilon_{cs}} + 2e^{\beta(h_s^+ - 2\epsilon_{cs})} + e^{\beta(2\epsilon_{cs} - h_s^-)} + e^{\beta(h_s^+ - h_s^- + \epsilon_{cs})} + e^{\beta(h_s^+ - h_s^-)} \quad (\text{A5})$$

When β is large, this sum is dominated by the term(s) with the largest exponent. Noticing that some terms are larger than others regardless of the parameters, we get

$$T_{C+S \rightarrow C+2P} \simeq 2e^{\beta(h_s^+ - \epsilon_{cs})} + e^{\beta \epsilon_{cs}} + e^{\beta(h_s^+ - h_s^- + \epsilon_{cs})} \quad (\text{A6})$$

The first term, with kinetic barrier $h_s^+ - \epsilon_{cs}$, is the time to cross the transition state and dissociate, which is reduced compared to the spontaneous reaction whose kinetic barrier is h_s^+ . The second term, with kinetic barrier ϵ_{cs} , corresponds to the time to release a monomer

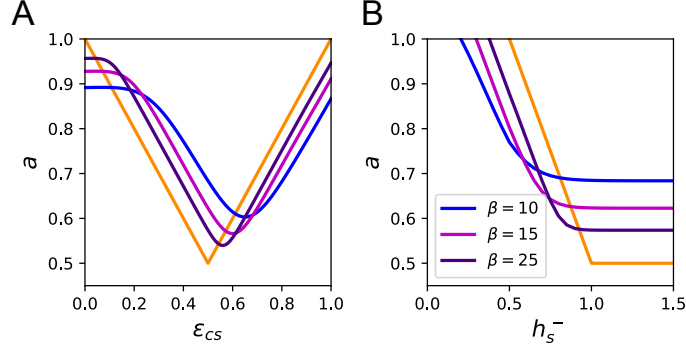


FIG. 6: Effective activation energy. The definition of the factor a by which the activation energy is reduced by catalysis, given in the low-temperature limit ($\beta \rightarrow \infty$) by Eq. (A1), can be extended to finite temperature as $a(\beta) = (\ln T_{C+S \rightarrow C+2P})/\beta$. **A.** Dependence of $a(\beta)$ on the interaction energy ϵ_{cs} . The orange curve reports $a = a(\beta = \infty)$ given by Eq. (A7). **B.** Dependence on the reverse activation energy h_s^- . These results are directly comparable to those of Fig. 2, since $\eta_{C+S \rightarrow C+2P} \sim e^{\beta(1-a)h_s^+}$.

from the catalyst. The last term, with kinetic barrier $h_s^+ - h_s^- + \epsilon_{cs}$, corresponds to an extra time due to recrossing the transition state while interacting with the catalyst.

This last term becomes irrelevant in the limit of an irreversible reaction where $h_s^- = \infty$. In this limit, there is a simple trade-off between the activation energy $h_s^+ - \epsilon_s$ and the release energy ϵ_{cs} : one decreases with ϵ_{cs} while the other increases. This trade-off, which is the essence of the Sabatier principle [17], implies an intermediate value for the optimal binding energy. In this model, the optimum is reached when the two kinetic barriers in the trade-off are equal, leading to an optimum with $\epsilon_{cs} = h_s^+/2$ and $T_{C+S \rightarrow C+2P} \sim 3e^{\beta h_s^+/2}$.

This optimum is unchanged for large but finite values of the reverse activation energy h_s^- up to the point where the third term in Eq. (A6) comes to dominate the second term, which occurs when $h_s^- < h_s^+$. The tradeoff is then between the first and third terms, with an optimal value reached for $\epsilon_{cs} = h_s^-/2$, in which case $T_{C+S \rightarrow C+2P} \sim 3e^{\beta(h_s^+ - h_s^-)/2}$. All in all, and as shown previously [3], the minimum mean first-passage time is of the form $T_{C+S \rightarrow C+2P} \sim e^{\beta a^* h_s^+}$, with

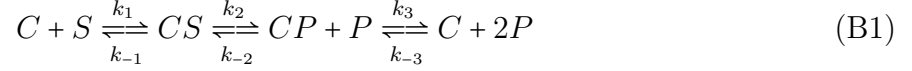
$$a^* = \max(1/2, 1 - h_s^-/h_s^+) \quad (\text{A7})$$

Two implications can be drawn from this calculation. First, since $a^* \geq 1/2$, this type of rigid catalysis can lower the activation barrier by at most a factor of 2. Second, catalysis requires a non-zero reverse barrier $h_s^- > 0$, otherwise $a = 1$. While these results are derived in the $\beta = \infty$ limit, they capture the dependence on the parameters ϵ_{cs} and h_s^- for finite values of β (Fig. 6).

Appendix B: Coarse-graining into a Markov model

The representation of the catalytic cycle given by Eq. (A2) differs in two respects from the representation of catalytic cycles by Markov chains usually presented in the literature. First, it includes unstable macrostates that cannot be treated as Markov states: for example, if we consider $\epsilon_{cs} < h_s^\pm$, as we did to obtain Eq. (3), $C:S^\ddagger$ is unstable because no activation

barrier separates it from the preceding and succeeding states. Second, it is derived in the limit where diffusion is instantaneous and therefore does not account for diffusion processes. One way to include them at a mean-field level is to assume mass-action kinetics. Eliminating unstable states and using mass action kinetics, Eq. (A2) is rewritten as



with

$$k_1 = k_d[S], \quad k_{-1} = \rho_{-1}, \quad k_2 = \rho_2/2, \quad k_{-2} = \rho_{-3}k_d[P], \quad k_3 = \rho_4, \quad k_{-3} = k_d[P] \quad (\text{B2})$$

where k_d is a diffusion coefficient and $[S]$ and $[P]$ are the concentrations of the dimers and monomers. With only two particles, these concentrations can take a limited number of values: $[S] = 0$ or $1/V$, $[P] = 0, 1/V$ or $2/V$. The factor 2 in $k_2 = \rho_2/2$ follows from $1/k_2 = 1/\rho_2 + 1/\rho_3 + \rho_{-2}/(\rho_2\rho_3) \simeq 2/\rho_2$, since $\rho_{-2} = \rho_3 = 1 \ll \rho_2$.

Ignoring the spontaneous reaction, the mean first-passage time $T_{C+S \rightarrow C+2P}$ is again obtained from this coarse-grained model using the general formula applicable to one-dimensional Markov chains (Appendix C),

$$T_{C+S \rightarrow C+2P} = \frac{1}{k_1} + \frac{1}{k_2} + \frac{1}{k_3} + \frac{k_{-1}}{k_1 k_2} + \frac{k_{-2}}{k_2 k_3} + \frac{k_{-1} k_{-2}}{k_1 k_2 k_3} \quad (\text{B3})$$

In the low temperature limit ($\beta \rightarrow \infty$), this formula gives results strictly equivalent to Eq. (A3).

Appendix C: Formulas relative to Markov processes

1. Transition matrix

Given the transition rates defined in Eq. (3), the master equation describes the evolution of the probability $\pi(x, t)$ for the system to be in configuration x at time t , namely

$$\partial_t \pi(x, t) = \sum_{y \neq x} (\pi(y, t) k(y \rightarrow x) - \pi(x, t) k(x \rightarrow y)) \quad (\text{C1})$$

It is convenient to represent this equation in matrix form. If L^2 is the number of lattice sites, then the number of configurations of the two particles is $N = L^2(L^2 - 1)$, and the time evolution can be represented by an N -dimensional vector $\pi(t)$ with components $\pi_x(t) = \pi(x, t)$. The master equation can then be rewritten

$$\partial_t \pi(t) = Q^T \pi(t) \quad (\text{C2})$$

where Q^T is the transpose of the $N \times N$ dimensional matrix Q whose components are

$$Q_{xy} = \begin{cases} k(x \rightarrow y) & \text{if } x \neq y \\ -\sum_{y \neq x} k(y \rightarrow x) & \text{if } x = y. \end{cases} \quad (\text{C3})$$

This transition matrix is known as the generator of the continuous time Markov chain.

2. Steady-state probabilities

The stationary distribution over the configurations is a N -dimensional vector π that can be obtained as the left-eigenvector of Q with eigenvalue 0, satisfying $\pi^\top Q = 0$, normalized to have $\sum_x \pi_x = 1$. If A is a set of configurations x , we denote by v_A a N -dimensional vector with $(v_A)_x = 1$ if $i \in A$ and 0 otherwise. The steady-state probability to be in state A is then $v_A^\top \pi$.

3. Mean first-passage times

Let A, B be two non-intersecting sets of configurations x . The mean first-passage time to reach B from a configuration $x \notin B$, denoted $\tau_{x \rightarrow B}$, is solution to $\sum_{y \notin B} Q_{xy} \tau_{y \rightarrow B} = -1$. The N -dimensional vector $\tau_{\cdot \rightarrow B}$ is therefore given by

$$\begin{aligned} \tau_{B \rightarrow B} &= 0 \\ \tau_{\bar{B} \rightarrow B} &= -(Q_{\bar{B}, \bar{B}})^{-1} u_{\bar{B}} \end{aligned} \quad (\text{C4})$$

where $u_{\bar{B}}$ is a vector whose dimension is the size of \bar{B} , with $(u_{\bar{B}})_x = 1$ for all x .

The global mean first-passage time from any configuration in A to B is $T_{A \rightarrow B} = \sum_{x \in A} \tau_{x \rightarrow B} / |A|$, where $|A|$ is the number of elements in A , i.e.,

$$T_{A \rightarrow B} = \frac{v_A^\top \tau_{A \rightarrow B}}{v_A^\top v_A} \quad (\text{C5})$$

4. Committors

The probability $c_x^{B < A}$ for a trajectory to reach B before A when starting from x is solution to $\sum_y Q_{xy} c_y^{B < A} = 0$ if $x \in I = \overline{A \cup B}$, with boundary conditions $c_x^{B < A} = 0$ if $x \in A$ and $c_x^{B < A} = 1$ if $x \in B$. We therefore have $Q_{I, I} c_I^{B < A} = -\sum_{y \in B} Q_{xy}$. In short, the N -dimensional vector $c^{B < A}$ is given by [19]

$$\begin{aligned} c_A^{B < A} &= 0 \\ c_B^{B < A} &= 1 \\ c_I^{B < A} &= -(Q_{I, I})^{-1} Q_{I, B} \quad (I = \overline{A \cup B}) \end{aligned} \quad (\text{C6})$$

At steady state, $1 - c^{B < A}$ also gives probability to have last been in A rather than in B .

5. Fluxes

The flux $\phi_{A \rightarrow B}$ is the number of first times at which B is reached after having visited A , divided by the total time. At steady state, the flux at which A transitions to B is the same as the flux at which B transitions to A . It is a scalar given by [19]

$$\phi_{A \leftrightarrow B} = \pi_A^\top Q_{A, \bar{A}} c_{\bar{A}}^{B < A} \quad (\text{C7})$$

6. Transition probabilities

At steady-state, the probability that the system is undergoing a transition from A to B is the probability that it has last visited A rather than B . It is a scalar given by [19]

$$\lambda_{A \rightarrow B} = \pi^\top (1 - c^{B < A}) = 1 - \pi^\top c^{B < A} \quad (\text{C8})$$

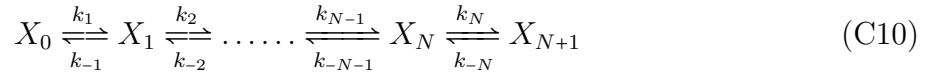
7. Rates

The rate from A to B is generally not the same as the rate from B to A . It is inverse of the mean time for a trajectory to reach B given that it last visited A . It is a scalar given by [19]

$$k_{A \rightarrow B} = \frac{\phi_{A \leftrightarrow B}}{\lambda_{A \rightarrow B}} \quad (\text{C9})$$

8. Mean first-passage times for one-dimensional Markov chains

The mean first passage time from X_0 to X_{N+1} through N intermediate states along a one-dimensional chain of transitions of the type



is given by

$$T_c = \sum_{j=1}^{N+1} \sum_{i=j}^{N+1} \frac{1}{k_j} \prod_{r=i}^{j-1} \frac{k_{-r}}{k_r} = \sum_{1 \leq i \leq j \leq N+1} \frac{k_{-i} k_{-(i+1)} \dots k_{-(j-2)} k_{-(j-1)}}{k_i k_{i+1} \dots k_{j-1} k_j}. \quad (\text{C11})$$

This result is for instance obtained by writing $T_c = \sum_{i=1}^N 1/k'_i$ where the times $1/k'_i$ are recursively defined by $1/k'_{N+1} = 1/k_{N+1}$ and $1/k'_i = (1 + k_{-i}/k'_{i+1})/k_i$ for $1 \leq i \leq N$, with $1/k'_i$ representing the mean residence time in state i [24].

-
- [1] O. Rivoire, Geometry and Flexibility of Optimal Catalysts in a Minimal Elastic Model., *The journal of physical chemistry. B*, vol. 124, pp. 807 – 813, 02 2020.
 - [2] M. Muñoz-Basagoiti, O. Rivoire, and Z. Zeravcic, Computational design of a minimal catalyst using colloidal particles with programmable interactions, *Soft Matter*, vol. 19, no. 21, pp. 3933–3939, 2023.
 - [3] O. Rivoire, How Flexibility Can Enhance Catalysis, *Physical Review Letters*, vol. 131, no. 8, p. 088401, 2023.
 - [4] L. Pauling, Nature of Forces between Large Molecules of Biological Interest, *Nature*, vol. 161, no. 4097, pp. 707–709, 1948.
 - [5] P. Sabatier, *La catalyse en chimie organique*. 1920.
 - [6] O. Rivoire, A role for conformational changes in enzyme catalysis, *Biophysical Journal*, vol. 123, no. 12, pp. 1563–1578, 2024.
 - [7] J. Šima, Catalysis of chemical processes: Particular teaching aspects, *African Journal of Chemical Education*, vol. 5, no. 2, pp. 2–15, 2015.

- [8] I. Chorkendorff and J. W. Niemantsverdriet, *Concepts of modern catalysis and kinetics*. John Wiley & Sons, 2017.
- [9] “Chemistry LibreTexts.” LibreTexts, <https://chem.libretexts.org> (accessed July 2024)
- [10] W. P. Jencks, Destabilization is as important as binding, *Philosophical Transactions of the Royal Society of London. Series A*, vol. 345, no. 1674, pp. 3–10, 1993.
- [11] A. Cornish-Bowden, *Fundamentals of enzyme kinetics*. John Wiley & Sons, 2013.
- [12] J. Ninio, Alternative to the steady-state method: derivation of reaction rates from first-passage times and pathway probabilities., *Proceedings of the National Academy of Sciences*, vol. 84, no. 3, pp. 663–667, 1987.
- [13] H. Qian, Cooperativity and Specificity in Enzyme Kinetics: A Single-Molecule Time-Based Perspective, *Biophysical Journal*, vol. 95, no. 1, pp. 10–17, 2008.
- [14] Y. Sakref, M. Muñoz-Basagoiti, Z. Zeravcic, and O. Rivoire, On Kinetic Constraints That Catalysis Imposes on Elementary Processes, *The Journal of Physical Chemistry B*, 2023.
- [15] A. Chatterjee and D. G. Vlachos, An overview of spatial microscopic and accelerated kinetic Monte Carlo methods, *Journal of Computer-Aided Materials Design*, vol. 14, no. 2, pp. 253–308, 2007.
- [16] D. J. Wales, Calculating rate constants and committor probabilities for transition networks by graph transformation, *The Journal of Chemical Physics*, vol. 130, no. 20, p. 204111, 2009.
- [17] A. J. Medford, A. Vojvodic, and J. S. Hummelshøj, From the Sabatier principle to a predictive theory of transition-metal heterogeneous catalysis, *Journal of Catalysis*, vol. 328, pp. 36 – 42, 00 2015.
- [18] J. B. S. Haldane, *Enzymes*. Longmans, Green & Co, 1930.
- [19] F. Noé, C. Schütte, E. Vanden-Eijnden, L. Reich, and T. R. Weigl, Constructing the equilibrium ensemble of folding pathways from short off-equilibrium simulations, *Proceedings of the National Academy of Sciences*, vol. 106, no. 45, pp. 19011–19016, 2009.
- [20] A. M. Berezhkovskii and A. Szabo, Committors, first-passage times, fluxes, Markov states, milestones, and all that, *The Journal of Chemical Physics*, vol. 150, no. 5, p. 054106, 2019.
- [21] W. P. Jencks, Binding energy, specificity, and enzymatic catalysis: the Circe effect, *Advances in Enzymology - and Related Areas of Molecular Biology*, vol. 43, pp. 219–410, 1975.
- [22] T. Omabegho, Allosteric linkages that model the chemical cycle of a molecular motor enzyme, *bioRxiv:2021.04.20.440673*, 2021.
- [23] Y. Sakref and O. Rivoire, Design principles, growth laws, and competition of minimal auto-catalysts, *Communications Chemistry* (in press), preprint arXiv:2403.19047, 2024.
- [24] J. Cao, Michaelis-Menten Equation and Detailed Balance in Enzymatic Networks, *The Journal of Physical Chemistry B*, vol. 115, no. 18, pp. 5493–5498, 2011.
- [25] In previous work [2], we included in the states S and $2P$ configurations in which one or two particles occupy a noninteracting binding site. For large volumes, the difference is negligible, but excluding the occupation of noninteracting binding sites allows a more meaningful comparison with the catalyzed reaction independent of volume.